Flow-Deformation Response of Dual-Porosity Media

By Derek Elsworth,[1] Member, ASCE, and Mao Bai[2]

ABSTRACT: A constitutive model is presented to define the linear poroelastic response of fissured media to determine the influence of dual porosity effects. A stress-strain relationship and two equations representing conservation of mass in the porous and fractured material are required. The behavior is defined in terms of the hydraulic and mechanical parameters for the intact porous matrix and the surrounding fracture system, allowing generated fluid pressure magnitudes and equilibration rates to be determined. Under undrained hydrostatic loading, the pore pressure–generation coefficients B, may exceed unity in either of the porous media or the fracture, representing a form of piston effect. Pressures generated within the fracture system equilibrate with time by reverse flow into the porous blocks. The equilibration time appears negligible for permeable sandstones, but it is significant for low-permeability geologic media. The constitutive model is represented in finite element format to allow solution for general boundary conditions where the influence of dual-porosity behavior may be examined in a global context.

INTRODUCTION

The linear flow-deformation behavior of geologic media is governed by the theory of single-porosity poroelasticity, as expounded originally by Biot (1941). Where, as in the case of fissured rock and soils, the medium comprises discrete fractions of differing solid compressibilities and permeabilities, a dual-porosity approach appears more appropriate.

The dual-porosity approach has been extensively developed to represent single-phase and multiphase flow in petroleum reservoirs. The original characterization of naturally fractured reservoirs by Warren and Root (1963) has been developed for radial flow in both blocky (Odeh 1965) and tabular reservoirs (Kazemi 1969) using analytical approaches and extended to multiphase flow using numerical techniques (Yamamoto et al. 1971; Kazemi et al. 1976; Kazemi and Merrill 1979; Thomas et al. 1983). Interest in single-phase behavior within dual-porosity reservoirs has been concerned with accurate representation of the flux fields within the porous and fractured components (Huyakorn et al. 1983) for application to mass (Bibby 1981) and thermal transport (Pruess and Narasimhan 1985; Elsworth 1989). In all of these applications it is assumed that total stresses remain constant with time, and therefore poroelastic effects are not incorporated.

The theory presented by Aifantis (1977, 1980) and Khaled et al. (1984) provides a suitable framework in which the flow-deformation behavior of dual-porosity media may be fully coupled to the deformation field as a multiphase continuum. Multiphase poroelasticity requires that the conditions of flow continuity within the different solid phases and the exchange between the phases are superimposed on the elastic displacement behavior of the fissured mass as body forces. As initially defined (Aifantis 1977), the constitutive coefficients describing the behavior of the aggregated medium

[1]Associate Professor, Dept. of Mineral Engrg., Pennsylvania State Univ., University Park, PA 16802.

[2]Research Associate, Dept. of Mineral Engrg., Pennsylvania State Univ., University Park, PA 16802. Now at School of Petroleum and Geological Engineering, University of Oklahoma, Norman OK 73019-0628.

defy direct physical interpretation. Although phenomenological coefficients describing both load-deformation and fluid-percolation response may be determined directly from laboratory and field testing of the fractured systems (Wilson and Aifantis 1982), these coefficients may be recovered more conveniently from basic knowledge of modulii and permeability of the components comprising matrix and fissure porosities.

Defining the response of the system directly in terms of the elastic and permeability properties of the components, with due regard for fissure geometry, offers the further advantage of ensuring that material nonlinearities of unknown magnitude are not inadvertently included within data reduced from field testing. This is an important factor, given long-standing knowledge on the nonlinear load-deformation behavior of interfaces (Goodman 1974) and the strong aperture dependence of fluid transmission in fissures (Iwai 1976). Indeed, the conditions needed to satisfy requirements for a linear theory of dual poroelasticity for fissured media may be so restrictive that, in all practicality, the phenomenon must be viewed as intrinsically nonlinear. This argument aside, only linear phenomena are considered in the following.

Where the structure of the fissured mass is well defined, as in the case of regularly jointed rocks and fissured soils, the contribution of fissure and matrix components to the overall flow and deformation response of the medium are readily apparent. Indeed, where elastic and flow properties of the fissures and matrix are known a priori, it is reasonable to develop the governing equations directly from this constituent basis. This exercise is completed in the following to develop the macroscopic continuum equations of linear poroelasticity on the basics of known fluid compressibility and defined fissure stiffness, porosities, and permeabilities.

CONSTITUTIVE EQUATIONS

The behavior of the dual porosity aggregate may be defined in terms of component equations representing the solid deformation and coupled fluid-pressure response. The morphology of the continuum is represented in Fig. 1.

Solid Deformation

The relationship between changes in total stresses ($\partial\sigma$) and intergranular stresses ($\partial\sigma'$) are governed by the Terzaghi (1928, 1943) relationship of the form
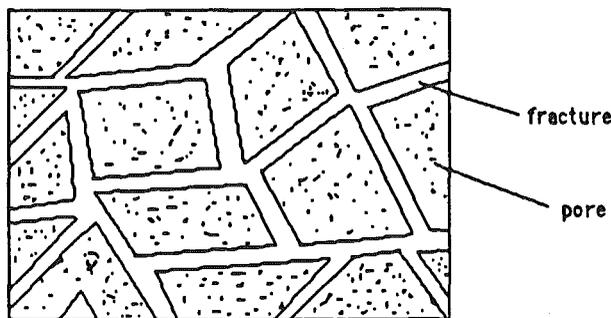

FIG. 1.   Morphology of Porous-Fractured Aggregate

108

$$\partial\boldsymbol{\sigma}_1 = \partial\boldsymbol{\sigma}_1' + \mathbf{m}\partial p_1 \quad\dotfill\quad (1a)$$

$$\partial\boldsymbol{\sigma}_2 = \partial\boldsymbol{\sigma}_2' + \mathbf{m}\partial p_2 \quad\dotfill\quad (1b)$$

where ∂p = change in fluid pressure. The effect of grain compression on the intergranular stresses are neglected. Stresses and strains are positive in compression. Subscripts 1 and 2 refer to the porous and fractured phases, respectively, and are represented as $\partial\boldsymbol{\sigma}_1 = \partial[\sigma_{xx}, \sigma_{yy}, \sigma_{zz}, \sigma_{xy}, \sigma_{xz}, \sigma_{yz}]_1^T$ and $\partial\boldsymbol{\sigma}_1 = \partial[\sigma_{xx}, \sigma_{zz}, \sigma_{xz}]_1^T$ for three-dimensional and two-dimensional problems, respectively. Since pore fluid pressures act on the normal stresses alone, the vector $\mathbf{m}^T$ is $[1,1,1,0,0,0]$ and $[1,1,0]$ in three- and two-dimensions. Vector or matrix quantities are represented by boldface type. It may be readily noted that the influence of grain compression on the intergranular stress relationship (Skempton 1960; Nur and Byerlee 1971) [(1)] may be accommodated by substituting a modified magnitude of the vector $\mathbf{m}$. This modified vector is determined as $\mathbf{m}_n = (\mathbf{m} - 1/3K_s\mathbf{D}_n\mathbf{m})$, where the subscript refers to the intergranular relation for the porous [$n = 1$ and $(1a)$] or fractured [$n = 2$ and $(1b)$] phases. In this, K_s is the bulk modulus of the solid and $\mathbf{D}_n$ is the elasticity matrix for phase n, as defined subsequently. The influence of grain compression on intergranular stresses are neglected because of the relative compressibility of the skeleton of interest in this study.

Local stress equilibrium requires that changes in total stress within adjacent phases must remain in equilibrium, such that

$$\partial\boldsymbol{\sigma}_1 = \partial\boldsymbol{\sigma}_2 = \partial\boldsymbol{\sigma} \quad\dotfill\quad (2)$$

The linear constitutive relationships for the separate phases are defined as

$$\partial\boldsymbol{\sigma}_1' = \mathbf{D}_1\partial\boldsymbol{\varepsilon}_1 \quad\dotfill\quad (3a)$$

$$\partial\boldsymbol{\sigma}_2' = \mathbf{D}_2\partial\boldsymbol{\varepsilon}_2 \quad\dotfill\quad (3b)$$

where $\boldsymbol{\varepsilon}$ = solid strain within each of the two materials, namely porous and fractured material, and the inverse relations recovered from $(3a,b)$ are

$$\partial\boldsymbol{\varepsilon}_1 = \mathbf{C}_1\partial\boldsymbol{\sigma}_1' \quad\dotfill\quad (4a)$$

$$\partial\boldsymbol{\varepsilon}_2 = \mathbf{C}_2\partial\boldsymbol{\sigma}_2' \quad\dotfill\quad (4b)$$

where $\mathbf{D}_n$ = the elasticity matrix for phase n with all other phases assumed rigid, and $\mathbf{C}_n$ = the compliance matrix under a similar arrangement, such that $\mathbf{D}_n^{-1} = \mathbf{C}_n$. Since $\mathbf{D}_n$ and $\mathbf{C}_n$ are written to represent the elastic behavior of phase n only, and are stated at a macroscopic level to contain a representative sample of matrix and fissure geometry, the total strain due to deformation in each of the phases is

$$\partial\boldsymbol{\varepsilon} = \partial\boldsymbol{\varepsilon}_1 + \partial\boldsymbol{\varepsilon}_2 \quad\dotfill\quad (5)$$

or, substituting (1) into (4) and recording the result into (5) gives

$$\partial\boldsymbol{\varepsilon} = (\mathbf{C}_1 + \mathbf{C}_2)\partial\boldsymbol{\sigma} - \mathbf{C}_1\mathbf{m}\partial p_1 - \mathbf{C}_2\mathbf{m}\partial p_2 \quad\dotfill\quad (6)$$

or

$$\partial\boldsymbol{\sigma} = \mathbf{D}_{12}(\partial\boldsymbol{\varepsilon} + \mathbf{C}_1\mathbf{m}\partial p_1 + \mathbf{C}_2\mathbf{m}\partial p_2) \quad\dotfill\quad (7)$$

where $\mathbf{D}_{12} = (\mathbf{C}_1 + \mathbf{C}_2)^{-1}$ and dividing through by time increment ∂t allows (7) to be recorded as

$$\dot{\boldsymbol{\sigma}} = \mathbf{D}_{12}(\dot{\boldsymbol{\varepsilon}} + C_1\mathbf{m}\dot{p}_1 + C_2\mathbf{m}\dot{p}_2) \quad \dots \dots \dots \dots \dots \dots \dots \dots \dots \quad (8)$$

representing the time-dependent load-deformation constitutive equation.

Fluid Pressure Response

Conservation of fluid mass must be maintained for each of the two porosity types, with appropriate transfer being possible between the two. The basic statement of continuity of flow requires that the divergence of the flow-velocity vector be equal to the rate of fluid accumulation per unit volume of space, i.e., $\nabla^T\mathbf{v}$ = rate of accumulation. Equating the continuity constraint for the porous phase with changes in fluid mass due to all possible mechanisms gives the rate of fluid accumulation as the summation of: (1) Change in total body strain resulting in fluid expulsion; (2) change in fluid pressure precipitating changes in volumetric pore fluid content as a result of fluid and grain compressibility; and (3) volumetric transfer between the porous blocks and the fractures under differential pressures. These three source terms represent the right-hand side of the continuity relationship as

$$\nabla^T\mathbf{v}_1 = \mathbf{m}^T\dot{\boldsymbol{\varepsilon}}_1 - \alpha_1\dot{p}_1 + K(p_1 - p_2) \quad \dots \dots \dots \dots \dots \dots \dots \dots \quad (9)$$

where $\nabla^T = (\partial/\partial x_1, \dots, \partial/\partial x_i)$ in the case of i dimensional geometry; Eulerian flow velocity $\mathbf{v}_1^T = [v_{x_1}, \dots, v_{x_i}]$ and $\alpha_1 = [n_1/K_f + (1 - n_1)/K_s]$, where n_1 = the porosity of phase 1; K_f = the fluid bulk modulus; and k_s = the solid grain bulk modulus. Transfer between the porous block and the surrounding fractures may be quantified by the assumption of a quasi-steady response governed by the coefficient K and the instantaneous pressure differential $(p_1 - p_2)$ (Warren and Root 1963).

In (9), the volume strain within the porous medium, $\mathbf{m}^T\boldsymbol{\varepsilon}_1$, refers to the drained condition where excess pore pressures are zero throughout the loading process. The proportion of the volume strain manifest within the porous phase may be determined from the total volume strain, $\mathbf{m}^T\boldsymbol{\varepsilon}_1$, by substituting (7) into (1) and the result into (4). This gives following division by ∂t, which

$$\mathbf{m}^T\dot{\boldsymbol{\varepsilon}}_1 = \mathbf{m}^TC_1\mathbf{D}_{12}(\dot{\boldsymbol{\varepsilon}} + C_1\mathbf{m}\dot{p}_1 + C_2\mathbf{m}\dot{p}_2) - \mathbf{m}^TC_1\mathbf{m}\dot{p}_1 \quad \dots \dots \dots \dots \quad (10)$$

which may be reduced to the drained response by requiring that $\dot{p}_1 = \dot{p}_2 = 0$. [The requirement of using drained solid body strain may be confirmed by noting the form of (40) where pressure changes are set to $\dot{p}_1 = \dot{p}_2 = 0$ leaving the only mechanism for fluid expulsion into the separate phases through displacement rates, $\dot{\mathbf{u}}$.] The truncated (drained) form of (10) may then be substituted into the continuity relationship of (9) to yield

$$\nabla^T\mathbf{v}_1 = \mathbf{m}^TC_1\mathbf{D}_{12}\dot{\boldsymbol{\varepsilon}} - \alpha_1\dot{p}_1 - K(p_1 - p_2) \quad \dots \dots \dots \dots \dots \dots \quad (11)$$

to give the final form of the continuity relationship for phase 1. Again, it is noted that the influence of grain compressibility as a result of changes in intergranular stresses has been neglected. This effect may, however, be incorporated by substituting the vector $\mathbf{m}_1$ for $\mathbf{m}$ in (11), where $\mathbf{m}_1$ accommodates the intergranular stress relationship of (1). This effect is small for the stress levels of interests within geotechnical engineering and may be neglected.

Repeating the same process for the fractured material gives a second continuity relationship

$$\nabla^T\mathbf{v}_2 = \mathbf{m}^TC_2\mathbf{D}_{12}\dot{\boldsymbol{\varepsilon}} - \alpha_2\dot{p}_2 + K(p_1 - p_2) \quad \dots \dots \dots \dots \dots \dots \quad (12)$$

where the fracture compressibility term is defined as $\alpha_2 = n_2/K_f$, with n_2

110

representing the fracture porosity. Again the influence of grain compressibility on the intergranular stress relationship is neglected, but it may be readily included by substituting $\mathbf{m}_2$ for $\mathbf{m}$.

DUAL-POROSITY LOAD RESPONSE

For the case of general loading, the dual-porosity response may be fully described by (8), (11), and (12) to determine the magnitude of instantaneously generated displacements and fluid pressures and their modification with time. Although these relationships are entirely general, it is instructive to consider the behavior under purely hydrostatic loading and examine the response in normalized format. This will allow us to determine the important differences between true dual-porosity systems and their representation by an equivalent single-porosity system.

Hydrostatic Behavior

Where a hydrostatic load is applied to the dual-porosity medium, the three-dimensional form of (7) that contains a total of six subordinate equations may be reduced to a single component. For a ubiquitously jointed medium containing orthogonal fractures of uniform spacing, s, the strain components may be reduced on noting that

$$\mathbf{m}^T \boldsymbol{\varepsilon} = 3\varepsilon \quad \dots\dots\dots\dots\dots\dots\dots\dots\dots\dots\dots\dots\dots\dots\dots\dots\dots \quad (13)$$

and the compliance matrices are represented as

$$C_1 = \frac{(1 - 2v)}{E} \quad \dots\dots\dots\dots\dots\dots\dots\dots\dots\dots\dots\dots\dots\dots \quad (14a)$$

$$C_2 = \frac{1}{k_n s} \quad \dots\dots\dots\dots\dots\dots\dots\dots\dots\dots\dots\dots\dots\dots\dots\dots \quad (14b)$$

where k_n = the joint normal stiffness and the stiffness matrix reduces to

$$D_{12} = (C_1 + C_2)^{-1} \quad \dots\dots\dots\dots\dots\dots\dots\dots\dots\dots\dots\dots\dots \quad (15)$$

Rearranging (8), (11), and (12) for an applied hydrostatic stress magnitude σ yields

$$\dot{\sigma} = D_{12}\dot{\varepsilon} + D_{12}C_1\dot{p}_1 + D_{12}C_2\dot{p}_2 \quad \dots\dots\dots\dots\dots\dots\dots\dots \quad (16)$$

$$K(p_1 - p_2) = 3D_{12}C_1\dot{\varepsilon} - \alpha_1\dot{p}_1 \quad \dots\dots\dots\dots\dots\dots\dots\dots \quad (17)$$

$$-K(p_1 - p_2) = 3D_{12}C_2\dot{\varepsilon} - \alpha_2\dot{p}_2 \quad \dots\dots\dots\dots\dots\dots\dots\dots \quad (18)$$

where a zero external flux condition ($\nabla^T \mathbf{v}_1 = \nabla^T \mathbf{v}_2 = 0$) has been applied as a further boundary condition. The behavior is most conveniently decomposed into: the undrained loading stage when fluid pressures p_{1_0} and p_{2_0} are generated; and the dissipation of pressures through fluid exchange in the subsequent drained behavior. The undrained pore pressures provide initial conditions to the initial value problem posed in (16)–(18). The magnitudes of undrained pore pressures may be evaluated, as discussed subsequently. Following undrained loading, dissipation begins under constant total stresses at the boundary where $\dot{\sigma} = 0$. Interest is restricted to the continuum level, where stress gradients are defined to be zero. Spatial changes in total stress that may occur within the volume, even under unchanged boundary stresses [see Mandel (1953)], are still admissible, but they require the additional

111

step of incorporating the equilibrium relationship introduced in (34). These considerations are in addition to the constitutive equations and our interest, for the moment, is merely in the constitutive relations. With some rearrangement, the governing equations [(16)–(18)] may be represented as

$$\dot{\varepsilon} = -C_1 \dot{p}_1 - C_2 \dot{p}_2 \quad \dots \dots \dots \dots \dots \dots \dots \dots \dots \dots \dots \dots \dots \quad (19)$$

$$\dot{p}_1 = -\frac{\gamma_{11}}{\gamma_{12}} (p_1 - p_2) \quad \dots \dots \dots \dots \dots \dots \dots \dots \dots \dots \dots \quad (20)$$

$$\dot{p}_2 = \frac{\gamma_{22}}{\gamma_{12}} (p_1 - p_2) \quad \dots \dots \dots \dots \dots \dots \dots \dots \dots \dots \dots \quad (21)$$

where

$$\gamma_{11} = \frac{K}{3D_{12}} \left(\frac{\alpha_{22}}{C_1} + 1 \right) \quad \dots \dots \dots \dots \dots \dots \dots \dots \dots \quad (22a)$$

$$\gamma_{22} = \frac{K}{3D_{12}} \left(\frac{\alpha_{11}}{C_2} + 1 \right) \quad \dots \dots \dots \dots \dots \dots \dots \dots \dots \quad (22b)$$

$$\gamma_{12} = (\alpha_{11}\alpha_{22} - C_1C_2) \quad \dots \dots \dots \dots \dots \dots \dots \dots \dots \dots \quad (22c)$$

$$\alpha_{11} = \left(\frac{\alpha_1}{3D_{12}C_1} + C_1 \right) \quad \dots \dots \dots \dots \dots \dots \dots \dots \dots \quad (22d)$$

$$\alpha_{22} = \left(\frac{\alpha_2}{3D_{12}C_2} + C_2 \right) \quad \dots \dots \dots \dots \dots \dots \dots \dots \dots \quad (22e)$$

Eqs. (20) and (21) are independent of the strain field and may be solved in time where boundary conditions are supplied directly. Solution to (20) and (21) may be determined as

$$p_1(t) = p_0 - (p_0 - p_{10})e^{-(\gamma_{11} + \gamma_{22})t/\gamma_{12}} \quad \dots \dots \dots \dots \dots \quad (23a)$$

$$p_2(t) = p_0 - (p_0 - p_{20})e^{-(\gamma_{11} + \gamma_{22})t/\gamma_{12}} \quad \dots \dots \dots \dots \dots \quad (23b)$$

where initial (undrained) conditions $p_1(0) = p_{10}$; $p_2(0) = p_{20}$ and terminal (fully drained) conditions $p_1(\infty) = p_2(\infty) = p_0$ control the response of the hydraulically closed system. The initial or undrained response occasioned upon application of a hydrostatic stress σ to the system may be evaluated by using the time-independent form of (16)–(18). Substituting the rearranged forms of (17) and (18) directly into (16) gives the instantaneous normalized strain $(D_{12}\varepsilon_0/\sigma)$ as

$$\frac{D_{12}\varepsilon_0}{\sigma} = \left(1 + \frac{3D_{12}C_1^2}{\alpha_1} + \frac{3D_{12}C_2^2}{\alpha_2} \right)^{-1} = \frac{1}{\beta_1} \quad \dots \dots \dots \dots \quad (24)$$

and the normalized pressure response is returned as

$$\frac{p_{10}}{\sigma} = \frac{3C_1}{\alpha_1\beta_1} = B_1 \quad \dots \dots \dots \dots \dots \dots \dots \dots \dots \dots \dots \quad (25)$$

112

$$\frac{p_{20}}{\sigma} = \frac{3C_2}{\alpha_2\beta_1} = B_2 \quad \dots\dots\dots\dots\dots\dots\dots\dots\dots\dots\dots\dots\dots\dots (26)$$

where these also are equivalent to Skempton's pore pressure coefficients, B_1 and B_2, written separately for the fluid in the pores and fractures. With some rearrangement, the pore pressure parameters may be defined as

$$B_1 = \frac{1}{\dfrac{\alpha_1}{3C_1} + \dfrac{\left(1 + \dfrac{\alpha_1}{\alpha_2}\dfrac{C_2^2}{C_1^2}\right)}{\left(1 + \dfrac{C_2}{C_1}\right)}} \quad \dots\dots\dots\dots\dots\dots\dots\dots\dots\dots\dots (27)$$

and

$$B_2 = \frac{1}{\dfrac{\alpha_2}{3C_2} + \dfrac{\left(1 + \dfrac{\alpha_2}{\alpha_1}\dfrac{C_1^2}{C_2^2}\right)}{\left(1 + \dfrac{C_1}{C_2}\right)}} \quad \dots\dots\dots\dots\dots\dots\dots\dots\dots\dots\dots (28)$$

The pore pressure parameters are no longer bounded between zero and unity, as is the magnitude of the instantaneous normalized strain, which represents the aggregated influence of effective stresses in the two phases. A large magnitude of β_1 suggests that the material will exhibit a small instantaneous strain, although the fluid pressures generated are further controlled by the magnitude of the porous or fracture compliances and the compressibility of the fluid as embodied in α_1 and α_2.

The long-term response of the system where $\nabla^T \mathbf{v}_1 = \nabla^T \mathbf{v}_2 = 0$ results in an equilibrium pore pressure distribution with $p_1 = p_2$ and a steady magnitude of normalized strain. These long-term equilibrium parameters $[p_1(\infty), p_2(\infty)$ and $\varepsilon(\infty)]$ are most easily recovered from solving the equivalent single-porosity problem, as follows.

EQUIVALENT SINGLE-POROSITY RESPONSE

The equations developed to describe the dual-porosity response may be modified to represent the case where it is assumed that pressures within both the porous and fractured material remain in equilibrium (i.e., $p_1 = p_2$). This is the assumption made when real porous-fractured systems are represented by a simple equivalent phase system. Requiring $p_1 = p_2$ for all times, including initial pressure p_{10} and p_{20}, then (16) reduces to

$$\dot{\sigma} = D_{12}\dot{\varepsilon} + \dot{p} \quad \dots\dots\dots\dots\dots\dots\dots\dots\dots\dots\dots\dots\dots (29)$$

and adding (17) and (18) under a similar requirement that $\dot{p}_1 = \dot{p}_2$, gives

$$3\dot{\varepsilon} = (\alpha_1 + \alpha_2)\dot{p} \quad \dots\dots\dots\dots\dots\dots\dots\dots\dots\dots\dots\dots (30)$$

where these represent the basic constitutive equations under hydrostatic loading. Implicit within (17) and (18), and by inference therefore in (30), is the requirement that $\nabla^T \mathbf{v} = 0$. Since no drainage is allowed, $\dot{\varepsilon}$ is zero

113

following loading with the result that fluid pressures are maintained at their initially induced magnitude. This differs from the true dual-porosity case where there is an interchange of fluid between the pores and fractures. In the usual manner, (29) and (30) may be premultiplied by dt and the limit taken as $dt \rightarrow 0$ to recover the instantaneous normalized strain and pore pressure magnitudes as

$$\frac{D_{12}\varepsilon_0}{\sigma} = \left(1 + \frac{3}{D_{12}(\alpha_1 + \alpha_2)}\right)^{-1} = \frac{1}{\beta_2} \quad \dots \dots \dots \dots \dots \dots \dots \quad (31)$$

and

$$\frac{P_0}{\sigma} = \frac{3}{D_{12}(\alpha_1 + \alpha_2)\beta_2} = \frac{1}{1 + \frac{D_{12}(\alpha_1 + \alpha_2)}{3}} = B \quad \dots \dots \dots \dots \dots \quad (32)$$

where again B is bounded by zero and unity and incorporates the compliance of the porous solid, the fracture, and the fluid together with the appropriate distribution of porosities within each of the phases.

PARAMETRIC RESPONSE

Under undrained loading, the instantaneous generation of pore pressures is controlled by B_1 and B_2 in the true dual-porosity system, and by B_0 in the pseudo dual-porosity system. For dual porosity, the mismatch in medium stiffness and porosity between the porous body and the fracture result in differential pressure generation that will diffuse with time to an equilibrium configuration. Where external drainage is controlled, the equilibrium pressure is given by $p/\sigma = B_0$ where this magnitude is intermediate to the instantaneous pore and fracture pressures.

Of significance are the magnitudes of instantaneous pore pressures in the pore and fracture as controlled by B_1 and B_2 of (25) and (26). Unlike B [(32)] for the pseudo dual-porosity system, the magnitude of B_1 and B_2 are not confined between zero and unity. Rather, one may be greater than unity and the complementary parameter less than unity. This behavior is representative of a piston effect, whereby pressures are amplified in the low stiffness porosity. According to (25) and (26), B_i is largest for large α_i/α_j and small C_i/C_j for $i = 1, 2; j = 1, 2$ and $i \neq j$, and also is controlled by the ratio α_i/C_i. Physically, pore pressure magnitudes are increased as porosity increases or as solid stiffness decreases. The influence is illustrated for a variety of sedimentary and crystalline rocks in Table 1. Porosities and stiffnesses have been added to augment available data for poroelastic behavior of single-porosity solids.

Regardless of fracture spacing, all materials return B_2 magnitudes close to or greater than unity for the fracture pressures and B_1 magnitudes of negligible proportion. Pore pressure parameter magnitudes for the aggregated system given by B in the table remain close to unity. As the fracture spacing is increased (from 0.1 m to 0.5 m), the aggregated B decreases uniformly due to the net increase in stiffness of the system. However, no similar generalization is possible for the coefficients B_1 and B_2.

The instantaneous pore pressure regime in the closed system ($\nabla^T \cdot v = 0$) is modified with time by diffusive exchange between the porous body and the fracture. For realistic parameter estimates, given in Table 1, dif-

114

TABLE 1. Material Properties

Parameter (1)	Ruhr sandstone (2)	Tennessee marble (3)	Charcoal granite (4)	Berea sandstone (5)	Westerly granite (6)	Weber sandstone (7)
$E(GPa)^a$	29.8	60.0	47.5	14.4	37.5	28.1
ν^a	0.12	0.25	0.27	0.20	0.25	0.15
$k_n(GPa \cdot m^{-1})^{b,d}$	12.1	83.0	83.0	12.1	83.0	12.1
$K_s(GPa)^a$	36.0	50.0	45.4	36.0	45.4	36.0
$K_f(GPa)^a$	3.3	3.3	3.3	3.3	3.3	3.3
$k_1(m)^b$	2×10^{-16}	1×10^{-19}	1×10^{-19}	1.9×10^{-13}	4×10^{-19}	1×10^{-15}
$\mu(GPa \cdot s)$	1×10^{-12}	1×10^{-12}	1×10^{-12}	1×10^{-12}	1×10^{-12}	1×10^{-12}
n_1^c	0.032	0.0052	0.014	0.064	0.00106	0.176
n_2	0.0032^e	0.052^f	0.05	0.0064^e	0.0106^f	0.0176^e
$s(m)$	0.1	0.1	0.1	0.1	0.1	0.1
B	0.986	0.912	0.905	0.982	0.941	0.969
B_1	8.5×10^{-4}	5.2×10^{-2}	4.9×10^{-2}	2.3×10^{-3}	1.9×10^{-2}	2.2×10^{-3}
B_2	1.031	1.018	1.029	1.050	1.104	1.028
$t_{50}(s)$	1.96×10^{-2}	2.08×10^{1}	2.44×10^{1}	2.40×10^{-5}	4.91×10^{0}	8.06×10^{-3}
$t_{95}(s)$	8.47×10^{-2}	8.98×10^{1}	1.05×10^{2}	1.06×10^{-4}	2.13×10^{1}	3.48×10^{-2}
$s(m)$	0.5	0.5	0.5	0.5	0.5	0.5
B	0.938	0.723	0.711	0.929	0.818	0.875
B_1	4.72×10^{-3}	2.47×10^{-1}	2.38×10^{-1}	1.34×10^{-2}	1.19×10^{-1}	1.20×10^{-2}
B_2	1.151	0.974	1.008	1.243	1.415	1.136
$t_{50}(s)$	3.72×10^{-1}	3.42×10^{2}	3.77×10^{2}	4.11×10^{-4}	5.88×10^{1}	1.49×10^{-1}
$t_{95}(s)$	1.61×10^{0}	1.43×10^{3}	1.63×10^{3}	1.78×10^{-3}	2.54×10^{2}	6.36×10^{-1}

[a]From Rice and Cleary (1976).
[b]From Witherspoon et al. (1980).
[c]From Touloukian et al. (1989).
[d]From Ryan et al. (1977).
[e]$n_2 = 0.1n_1$ for sedimentary rock.
[f]$n_2 = 10.0n_1$ for crystalline and metamorphic rock.

115

fusion is most likely from the fractures into the circumscribed blocks. The rate of this process may be considered as an indication of the relative importance of the dual-porosity effect. The equilibration rate is controlled by a dimensionless time given in (23a) and (23b) as $t_D = (\gamma_{11} + \gamma_{22})t/\gamma_{12}$, whereby the time to 50% and 95% equilibration of pressures are given by $t_D^{50} = 0.6931$ and $t_D^{95} = 2.9957$. In terms of the physical parameters of the system

$$t_D = \frac{K\left(\dfrac{\alpha_{22}}{C_1} + \dfrac{\alpha_{11}}{C_2} + 2\right)t}{3D_{12}(\alpha_{11}\alpha_{22} - C_1 C_2)} \quad \dots\dots\dots\dots\dots\dots\dots\dots\dots\dots\dots\dots\dots\dots \quad (33)$$

where, in addition to the material coefficients controlling deformation, the block permeability, k_i, and appropriate diffusion lengths are incorporated.

The behavior of representative sandstones in Table 1 are characterized by very rapid response times, reaching t^{95} in less than a second. The low-permeability matrix of the crystalline rock impedes equilibration that, dependent on permeability and fracture spacing, may extend over thousands of seconds. Characteristic responses are illustrated in Fig. 2 to illustrate the form of the response. With drainage potential proportional to fracture spacing s^2, flatter responses in time are elicited where the path length is increased.

Although parametric analyses previously were limited to sandstones and crystalline rock, the major trends in behavior are apparent. Firstly, fluid pressures developed in compliant fractures may considerably exceed those developed in the porous body. These differential pressures will only be significant, however, if matrix permeabilities are sufficiently low that the pressure differential may be sustained in time. From the time scales apparent for permeable (sandstones) and impermeable (crystalline) materials, it appears that dual-porosity effects may be of little consequence in permeable media, but drainage time scales are sufficient in low-permeability rocks to cause noticeable effect. Where permeability controls behavior, clays and low-permeability silts may be subject to dual-porosity effects.
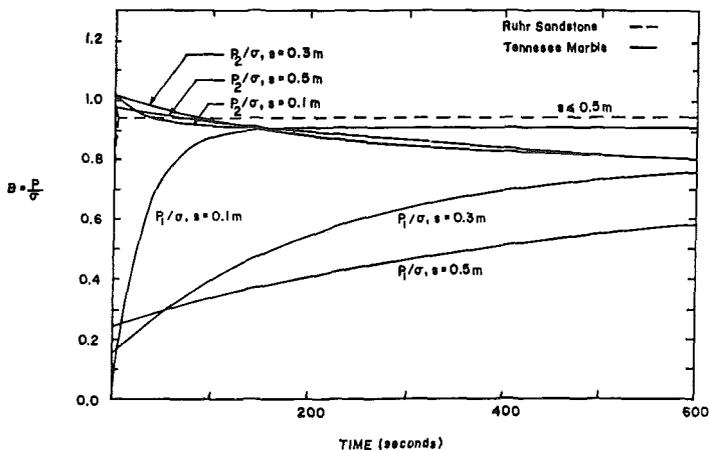

FIG. 2. Undrained Pore Pressure Response for Fractured Sandstone and Fractured Marble

116

GLOBAL BEHAVIOR

It is possible to solve a broader range of problems only if the previously developed constitutive behaviors are globally framed to represent spatial interaction. This requires that the constitutive, load-deformation relationship of (7) is substituted into an equilibrium statement and that the flow continuity (11) and (12) have an appropriate constitutive equation applied. The constitutive relationship, in this instance, is supplied by Darcy's law (Bear 1972).

For the general representation of heterogeneous, mixed–initial value problems, the finite element method is chosen. The equilibrium statement in its most general form is given as

$$\int_v \mathbf{B}^T \partial \boldsymbol{\sigma} \, dV - \partial \mathbf{f} = 0 \dotfill (34)$$

where $\mathbf{B}$ = the strain-displacement matrix; $\partial \mathbf{f}$ = an incremental vector of applied boundary tractions, and the integration is completed over the volume of the domain (dV). Defining all quantities in terms of nodal variables

$$\partial \boldsymbol{\varepsilon} = \mathbf{B} \partial \mathbf{u} \dotfill (35a)$$

$$\partial p_1 = \mathbf{N} \partial \mathbf{p}_1 \dotfill (35b)$$

$$\partial p_2 = \mathbf{N} \partial \mathbf{p}_2 \dotfill (35c)$$

where $\partial \mathbf{u}$ = a vector of incremental nodal displacements; $\partial \mathbf{p}$ = a vector of nodal pressures; and $\mathbf{N}$ = a vector of shape functions interpolating fluid pressures. Substituting (7) and (35) into (34), dividing by ∂t, and rearranging gives the incremental equation in finite element format as

$$\int_v \mathbf{B}^T \mathbf{D}_{12} \mathbf{B} \, dV \, \dot{\mathbf{u}} + \int_v \mathbf{B}^T \mathbf{D}_{12} \mathbf{C}_1 \mathbf{m} \mathbf{N} \, dV \, \dot{\mathbf{p}}_1$$

$$+ \int_v \mathbf{B}^T \mathbf{D}_{12} \mathbf{C}_2 \mathbf{m} \mathbf{N} \, dV \, \dot{\mathbf{p}}_2 = \dot{f} \dotfill (36)$$

where a superscript dot identifies time derivative.

Darcy's law must be added to the continuity requirements already imposed in (11) and (12) and may be simply stated as

$$\mathbf{v}_1 = \frac{-k_1}{\mu} \nabla(p_1 + \gamma Z) \dotfill (37)$$

where γ = the unit weight of the fluid; μ = the dynamic viscosity; k_1 = the porous medium permeability with the fracture permeability set to zero; and Z = the elevation of the control volume. Substituting (37) into (11) and applying the Galerkin principle results in

$$-\frac{1}{\mu} \int_v \mathbf{A}^T \mathbf{k}_1 \mathbf{A} \, dV \, \mathbf{p}_1 + \int_v \mathbf{N}^T \mathbf{m}^T \mathbf{C}_1 \mathbf{D}_{12} \mathbf{B} \, dV \, \dot{\mathbf{u}} - \alpha_1 \int_v \mathbf{N}^T \mathbf{N} \, dV \, \dot{\mathbf{p}}_1$$

$$- K \int_v \mathbf{N}^T \mathbf{N} \, dV (\mathbf{p}_1 - \mathbf{p}_2) = \frac{\gamma}{\mu} \int_v \mathbf{A}^T \mathbf{k}_1 \mathbf{A} \, dV \, \mathbf{Z} \dotfill (38)$$

for the porous phase and for the fractured medium

117

$$-\frac{1}{\mu}\int_v \mathbf{A}^T\mathbf{k}_2\mathbf{A}\,dV\,\mathbf{p}_2 + \int_v \mathbf{N}^T\mathbf{m}^T\mathbf{C}_2\mathbf{D}_{12}\mathbf{B}\,dV\,\dot{\mathbf{u}} - \alpha_2\int_v \mathbf{N}^T\mathbf{N}\,dV\,\dot{\mathbf{p}}_2$$

$$+\,K\int_v \mathbf{N}^T\mathbf{N}\,dV(\mathbf{p}_1 - \mathbf{p}_2) = \frac{\gamma}{\mu}\int_v \mathbf{A}^T\mathbf{k}_2\mathbf{A}\,dV\,\mathbf{Z}\,\dotfill \text{(39)}$$

where $\mathbf{k}_2 =$ a matrix of fracture permeabilities.

Eqs. (36), (38), and (39) may be written at any time level (say, $t + \Delta t$) and are most conveniently represented in matrix form as

$$\begin{bmatrix} 0 & 0 & 0 \\ 0 & (-\mathbf{K}_1 - \mathbf{S}_3) & \mathbf{S}_3 \\ 0 & \mathbf{S}_3 & (-\mathbf{K}_2 - \mathbf{S}_3) \end{bmatrix} \begin{bmatrix} \mathbf{u} \\ \mathbf{p}_1 \\ \mathbf{p}_2 \end{bmatrix}^{t+\Delta t}$$

$$+ \begin{bmatrix} \mathbf{F} & \mathbf{G}_1 & \mathbf{G}_2 \\ \mathbf{E}_1 & -\mathbf{S}_1 & 0 \\ \mathbf{E}_2 & 0 & -\mathbf{S}_2 \end{bmatrix} \begin{bmatrix} \dot{\mathbf{u}} \\ \dot{\mathbf{p}}_1 \\ \dot{\mathbf{p}}_2 \end{bmatrix}^{t+\Delta t} = \begin{bmatrix} \dot{\mathbf{f}} \\ \mathbf{K}_1\gamma\mathbf{Z} \\ \mathbf{K}_2\gamma\mathbf{Z} \end{bmatrix}^{t+\Delta t} \dotfill \text{(40)}$$

where all submatrices are defined in Appendix I.

These coupled equations remain symmetric, but they must be rearranged prior to solution in time. All terms on the right-hand side are known. The matrix relation may be integrated in time by using any convenient representation of the time derivatives. Using a fully implicit scheme, such that

$$\dot{\mathbf{u}}^{t+\Delta t} = \frac{1}{\Delta t^{t+\Delta t}}(\mathbf{u}^{t+\Delta t} - \mathbf{u}^t) \dotfill \text{(41a)}$$

$$\dot{\mathbf{p}}_1^{t+\Delta t} = \frac{1}{\Delta t^{t+\Delta t}}(\mathbf{p}_1^{t+\Delta t} - \mathbf{p}_1^t) \dotfill \text{(41b)}$$

$$\dot{\mathbf{p}}_2^{t+\Delta t} = \frac{1}{\Delta t^{t+\Delta t}}(\mathbf{p}_2^{t+\Delta t} - \mathbf{p}_2^t) \dotfill \text{(41c)}$$

and substituting (41) into (40) gives

$$\frac{1}{\Delta t^{t+\Delta t}}\begin{bmatrix} \mathbf{F} & \mathbf{G}_1 & \mathbf{G}_2 \\ \mathbf{E}_1 & (-\mathbf{K}_1\Delta t^{t+\Delta t} - \mathbf{S}_1 - \Delta t\mathbf{S}_3) & \Delta t\mathbf{S}_3 \\ \mathbf{E}_2 & \Delta t\mathbf{S}_3 & (-\mathbf{K}_2\Delta t^{t+\Delta t} - \mathbf{S}_2 - \Delta t\mathbf{S}_3) \end{bmatrix}$$

$$\begin{bmatrix} \mathbf{u} \\ \mathbf{p}_1 \\ \mathbf{p}_2 \end{bmatrix}^{t+\Delta t} = \frac{1}{\Delta t^{t+\Delta t}}\begin{bmatrix} \mathbf{F} & \mathbf{G} & \mathbf{G}_2 \\ \mathbf{E}_1 & -\mathbf{S}_1 & 0 \\ \mathbf{E}_2 & 0 & -\mathbf{S}_2 \end{bmatrix}\begin{bmatrix} \mathbf{u} \\ \mathbf{p}_1 \\ \mathbf{p}_2 \end{bmatrix}^t + \begin{bmatrix} f \\ \mathbf{K}_1\gamma\mathbf{Z} \\ \mathbf{K}_2\gamma\mathbf{Z} \end{bmatrix}^{t+\Delta t} \dotfill \text{(42)}$$

where the matrix comprising the left-hand side is time invariant if a constant time-step magnitude is chosen. Initial undrained conditions are recovered if $\mathbf{K}_1 = \mathbf{K}_2 = 0$ and $K = 0$ allowing (42) to be solved for $\mathbf{u}$, $\mathbf{p}_1$ and $\mathbf{p}_2$.

A two-dimensional formulation is chosen to illustrate the potential of the dual-porosity formulation. Suitable shape functions must be chosen to represent the quadratic displacement field and bilinear fluid pressure variation present within individual elements. A four-node quadrilateral isoparametric element with quadratic-incompatible modes is used. The incompatible modes are condensed out at the element level.

The broad range of material parameters that influence the pressure generation and dissipation response makes meaningful representation of transient behavior difficult. The versatility of the proposed technique is illus-

118

trated for a one-dimensional column for the parameters reported in Table 2. The fluid pressure response with depth is illustrated in Fig. 3 for a fracture spacing, s, of 0.1 m. Fluid pressures generated within the fractures are considerably greater than the matrix pore pressures. With time, the fracture pressures dissipate into the porous blocks until an equilibrium is reached. In this example, following the establishment of an equilibrium pressure distribution, the consolidation process will continue by drainage from the top of the layer. The surface settlement associated with the expulsion of fluid from the dual-porosity system is illustrated in Fig. 4. Fracture spacings of 0.025, 0.05, and 0.1 m are used to demonstrate the differing responses. Where spacing is decreased, the dissipation process is accelerated. The dual-porosity response is contrasted with the behavior of a single-porosity system, where the different form of settlement-versus-time behavior is apparent.

A two-dimensional geometry, represented in Fig. 5, also may be used to illustrate the essential differences between single-porosity and dual-porosity effects. The response to a load of finite extent is illustrated in Fig. 6. As fracture spacing is decreased, the magnitude of initial normalized displacement increases, reflecting the dominant influence of fracture stiffnesses on the deformation behavior. The small block dimensions present within the

TABLE 2. Example Coefficients

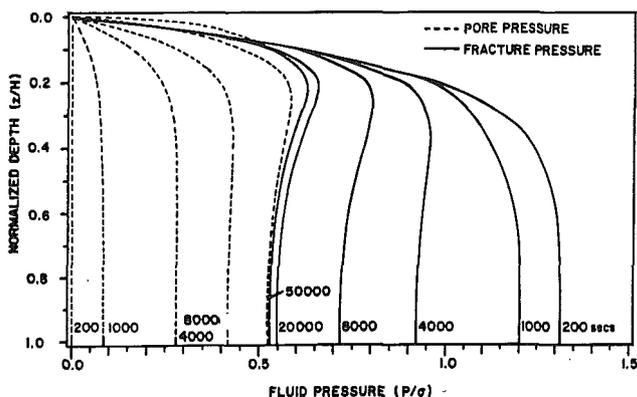| Parameter (1)	Definition (2)	Magnitude (3)	Units (4)
E	modulus of elasticity	1.0	MN/m^2
ν	Poisson's ratio	0.15	
k_n	fissure stiffness	0.1	MN/m^2/m
K_f	fluid bulk modulus	0.1	MN/m^2
n_1	matrix porosity	0.1	
n_2	fissure porosity	0.05	
k_1/μ	matrix permeability	0.01×10^{-3}	m^4/(MN · s)
k_2/μ	fissure permeability	0.1	m^4/(MN · s)
s	fissure spacing	0.025, 0.05, 0.1	m

FIG. 3. Pore Pressure Equilibration Response for One-Dimensional Column Loaded Axially
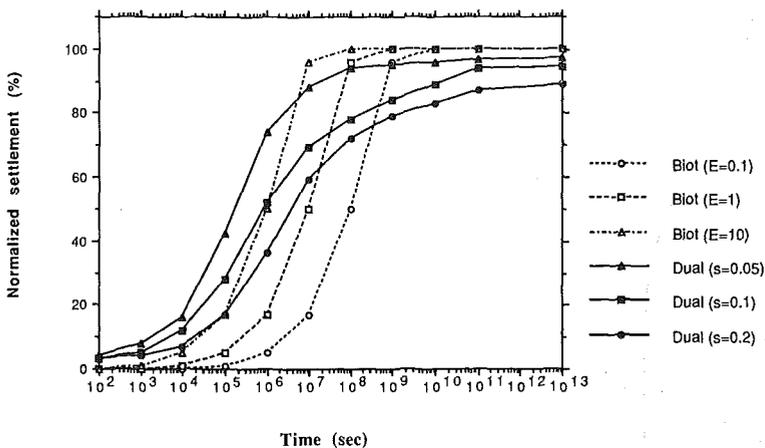
119

FIG. 4. Surface Displacement Response for One-Dimensional Column Loaded Axially
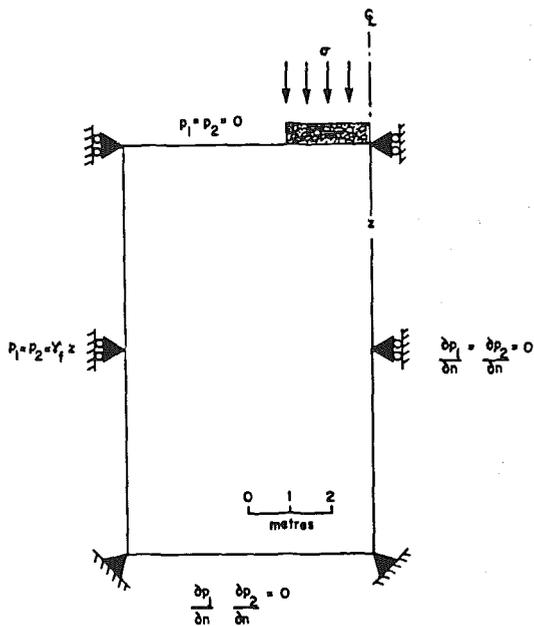

FIG. 5. Two-Dimensional Geometry

closely fractured medium result in an acceleration of the consolidation process. As bulk permeability magnitude is correspondingly increased, the dual-porosity behavior exhibits a characteristic acceleration in the early time response and a deceleration in the late time response over the equivalent single-porosity behavior. The former characteristic results from the rapid equilibrating of fluid pressures within the fractures where dissipation in-

120

creases the magnitude of effective stresses. The high compressibility of the fractures correspondingly yields a magnified response. At later times, the dual porosity exhibits a more sluggish response over the equivalent single-porosity behavior as a result of delayed changes in effective stresses within the porous blocks. This behavior is slightly magnified in time as block dimension is increased, resulting in a longer dissipation tail, as evident in Fig. 6.

CONCLUSIONS

A constitutive model for the coupled flow-deformation response of dual-porosity media has been presented. The formulation is stated in component terms, where behavior is controlled by the mechanical and hydraulic response of the individual porous and fractured phases. Representation in this form allows the potential importance of dual-porosity effects to be evaluated in controlling the coupled flow-deformation behavior of fractured geologic media.

Pore pressure coefficients B_1 and B_2 may be defined for the dual-porosity response, where the magnitudes are not necessarily confined to the range between zero and unity. For realistic material parameters, the magnitude of the pore pressure coefficient for the fractures is commonly greater than unity, and for the porous medium, less than unity. With the generation of this pressure differential, fluid transfer between the porous medium and the fracture will attempt to equilibrate the pressures. Equilibration times are controlled by the compliances of the porous medium and the fractures, together with porosities and the block-fracture fluid-transfer coefficient K. This latter component is a function of block size and block permeability. Where undrained loading is prescribed, the times to 50% and 95% equilibration may be determined explicitly.

Where general boundary conditions are applied to the dual-porosity system, a numerical solution method must be employed, Representation as a finite element system is particularly appropriate, allowing spatial variability in parameters and general boundary conditions to be readily accommodated.
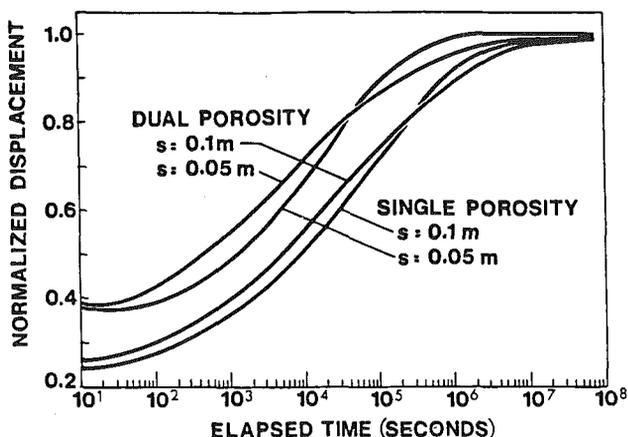

FIG. 6. Surface Displacement Response at Centerline for Single-Porosity and Dual-Porosity Systems (parameters Given in Table 2)

121

The procedure may be applied to a variety of engineering situations where the accurate determination of parameters associated with dual-porosity systems is important. These include the performance of fractured clay tills used as barriers to contaminated ground water and waste leachate and the behavior of fractured rocks deforming above mined underground openings. In either instance, the behavior of the dual-porosity medium is distinctively different from that of a single-porosity continuum, and it is important to recognize this differentiation if serviceable designs are to be commissioned. For example, large initial deformations are apparent in the dual-porosity medium under undrained loading that result in considerably different transient response to anything that can be explained using single-porosity representation. Thus, use of an incorrect phenomenological model in describing field data would erroneously predict the performance of the prototype. For this reason, it is imperative that a correct and adequate model is initially selected.

ACKNOWLEDGMENTS

APPENDIX I.   SUBMATRICES

$$E_1 = \int_v N^T m^T C_1 D_{12} B \; dV \quad \dots\dots\dots\dots\dots\dots\dots\dots\dots\dots\dots\dots (43)$$

$$E_2 = \int_v N^T m^T C_2 D_{12} B \; dV \quad \dots\dots\dots\dots\dots\dots\dots\dots\dots\dots\dots\dots (44)$$

$$F = \int_v B^T D_{12} B \; dV \quad \dots\dots\dots\dots\dots\dots\dots\dots\dots\dots\dots\dots\dots\dots (45)$$

$$G_1 = \int_v B^T D_{12} C_1 m N \; dV \quad \dots\dots\dots\dots\dots\dots\dots\dots\dots\dots\dots\dots (46)$$

$$G_2 = \int_v B^T D_{12} C_2 m N \; dV \quad \dots\dots\dots\dots\dots\dots\dots\dots\dots\dots\dots\dots (47)$$

$$H = \int_v N^T N \; dV \quad \dots\dots\dots\dots\dots\dots\dots\dots\dots\dots\dots\dots\dots\dots\dots (48)$$

$$K_1 = \frac{1}{\mu} \int_v A^T k_1 A \; dV \quad \dots\dots\dots\dots\dots\dots\dots\dots\dots\dots\dots\dots\dots (49)$$

$$K_2 = \frac{1}{\mu} \int_v A^T k_2 A \; dV \quad \dots\dots\dots\dots\dots\dots\dots\dots\dots\dots\dots\dots\dots (50)$$

$$S_1 = \alpha_1 H \quad \dots\dots\dots\dots\dots\dots\dots\dots\dots\dots\dots\dots\dots\dots\dots\dots\dots (51)$$

$$S_2 = \alpha_2 H \quad \dots\dots\dots\dots\dots\dots\dots\dots\dots\dots\dots\dots\dots\dots\dots\dots\dots (52)$$

$$S_3 = KH \quad \dots\dots\dots\dots\dots\dots\dots\dots\dots\dots\dots\dots\dots\dots\dots\dots\dots\dots (53)$$

122

APPENDIX II. REFERENCES

Aifantis, E. C. (1977). "Introducing a multi-porous medium." *Developments in mechanics*, 8, 209–211.

Aifantis, E. C. (1980). "On the problem of diffusion in solids." *Acta Mechanica*, 37, 265–296.

Bear, J. (1971). *Dynamics of fluids in porous media*. American Elsevier, New York, N.Y.

Bibby, R. (1981). "Mass transport of solutes in dual porosity media." *Water Resour. Res.*, 17, 1075–1081.

Biot, M. A. (1941). "General theory of three-dimensional consolidation." *J. Appl. Phys.* 12, 151–164.

Elsworth, D. (1989). "Thermal permeability enhancement of blocky rocks: one dimensional flows." *Int. J. Rock Mech. Min. Sci. Geomech. Abstr.*, 26(3/4), 329–339.

Goodman, R. E. (1974). "The mechanical properties of joints." *Proc. of the Third Congress of Int. Soc. for Rock Mech.*, 127–140.

Huyakorn, P. S., Lester, B. H., and Faust, C. R. (1983). "Finite element techniques for modeling groundwater flow in fractured aquifers." *Water Resour. Res.*, 19, 1019–1035.

Iwai, K. (1976). "Fundamental studies of fluid flow through a single fracture," thesis presented to the University of California, at Berkeley, California, in partial fulfillment of the requirements of the degree of Doctor of Philosophy.

Kazemi, H. (1969). "Pressure transient analysis of naturally fractured reservoirs with uniform fracture distribution." *Soc. Pet. Engrg. J.*, 9, 451–462.

Kazemi, H., Merrill, L. S., Jr., Porterfield, K. L., and Zeman, P. R. (1976). "Numerical simulation of water-oil flow in naturally fractured reservoirs." *Soc. Pet. Engrg. J.*, 16, 317–326.

Kazemi, H., and Merrill, L. S. Jr. (1979). "Numerical simulation of water imbibition in fractured cores." *Soc. Pet. Engrg. J.*, 19, 175–182.

Khaled, M. Y., Beskos, D. E., and Aifantis, E. C. (1984). "On the theory of consolidation with double porosity—III. A finite element formulation." *Int. J. Numer. Anal. Meth. Geomech.*, 8, 101–123.

Mandel, J. (1953). "Consolidation des sols (étude mathematique)." *Geotechnique*, 3, 287–299.

Nur, A., and Byerlee, J. D. (1971). "An exact effective stress law for elastic deformation of rock with fluids." *J. Geophys. Res.*, 76(26), 6414–6419.

Odeh, A. S. (1965). "Unsteady-state behavior of naturally fractured reservoirs." *Soc. Pet. Engrg. J.*, 5, 60–66.

Pruess, K., and Narasimhan, T. N. (1985). "A practical method for modelling fluid and heat flow in fractured porous media." *Soc. Pet. Engrg. J.*, 25, 14–26.

Rice, J. R., and Cleary, M. P. (1976). "Some basic stress diffusion solutions for fluid saturated elastic media with compressible constituents." *Rev. Geophys. Space Phys.*, 14(2), 227–241.

Ryan, T. M., Farmer, I., and Kimbrell, A. F. (1977). "Laboratory determination of fracture permeability." *Proc. of the 18th U.S. Symp. on Rock Mechanics*,

Skempton, A. W. (1960). "Effective stress in soils, concrete and rock." *Proc. of the Symp. on Pore Pressure and Suction in Soils*, Butterworths, London, U.K., 1.

Terzaghi, K. (1923). "Die Berechnung der Durchasigkeitsziffer des Tones aus dem Verlauf der hydrodynamishen Spannungserscheinungen, Sitzungsber." *Acad. Wiss. Wien Math Naturwiss.* K1. Alot. 2A, 132, 105 (in German).

Terzaghi, K. (1943). *Theoretical soil mechanics*, John Wiley & Sons, New York, N.Y.

Thomas, L. K., Dixon, N. T., and Pierson, G. R. (1983). "Fractured reservoir simulation." *Soc. Pet. Engrg. J.*, 23, 42–54.

Touloukian, Y. S., Judd, W. R., and Roy, R. F. (1989). *Physical properties of rocks and minerals*. 11(2), McGraw-Hill, New York, N.Y.

Warren, J. E., and Root, P. J. (1963). "The behavior of naturally fractured reservoirs." *Soc. Pet. Engrg. J.*, 3, 245–255.

123

Wilson, R. K., and Aifantis, E. C. (1982). "On the theory of consolidation with double porosity." *Int. J. Engrg. Sci.*, 20(9), 1009–1035.

Witherspoon, P. A., Wang, J. S. Y., Iwai, K., and Gale, J. E. (1980). "Validity of cubic law for fluid flow in a deformable structure." *Water Resour. Res.*, 16(16), 1016–1024.

Yamamoto, R. H., Padgett, J. B., Ford, W. T., and Boubeguira, A. (1971). "Compositional reservoir simulator for fissured systems—the single block model." *Soc. Pet. Engrg. J.*, 11, 113–128.

APPENDIX III. NOTATION

The following symbols are used in this paper:

A = derivatives of shape function matrix $\mathbf{N}$;
$\mathbf{B}$ = strain displacement matrix;
B_i = Skempton's fluid pressure coefficients in true dual-porosity system;
B = Skempton's fluid pressure coefficients in pseudodual-porosity system;
$\mathbf{C}_i$ = compliance matrices;
$\mathbf{D}_i$ = elasticity matrices;
$\mathbf{D}_{12}$ = elasticity matrix $(\mathbf{C}_1 + \mathbf{C}_2)^{-1}$;
E = Young's modulus;
$\mathbf{f}$ = vector of boundary tractions;
K = fluid transfer coefficient;
k_i = permeabilities;
k_n = joint normal stiffness;
K_f = fluid bulk modulus;
K_s = solid grain bulk modulus;
$\mathbf{m}$ = one dimensional vector; for three-dimensional problem, $m^T = (1\ 1\ 1\ 0\ 0\ 0)$; for two-dimensional problem, $m^T = (1\ 1\ 0)$;
$\mathbf{m}_i$ = modified intergranular stress relationship;
$\mathbf{m}_n$ = $(\mathbf{m} - 1/3Ks\mathbf{D}_n\mathbf{m})$;
n_i = porosities;
p_i = fluid pressure;
s = fracture spacing;
t = time;
t_D = dimensionless time;
$\mathbf{u}$ = displacement vector;
$\mathbf{v}_i$ = flow velocity vector;
Z = elevation of control volume;
∂ = partial differential operator;
α_i = hydrostatic compressibility;
γ = unit weight of fluid;
∂ = partial differential operator;
ε = strain vector; in three-dimensional Cartesian coordinates, $\varepsilon^T = (\varepsilon_{xx}\varepsilon_{yy}\varepsilon_{zz}\gamma_{xy}\gamma_{xz}\gamma_{yz})$;
μ = dynamic viscosity;
ν = Poisson ratio; and
σ = stress vector; in three-dimensional Cartesian coordinates, $\sigma^T = (\sigma_{xx}\sigma_{yy}\sigma_{zz}\sigma_{xy}\sigma_{xz}\sigma_{yz})$.

Subscripts

i = 1, 2, denoting pore phase and fracture phase, respectively.

124